12th AIAA Aviation Technology, Integration, and Operations (ATIO) Conference and 14th AIAA/ISSM
17 - 19 September 2012, Indianapolis, Indiana

AIAA 2012-5430

Impact of Different Wake Models On the Estimation of Wind Farm Power Generation

Weiyang Tong*
Syracuse University, Syracuse, NY, 13244
Souma Chowdhury† and Jie Zhang†
Rensselaer Polytechnic Institute, Troy, New York 12180
Achille Messac,‡
Syracuse University, Syracuse, NY, 13244

The power generation of a wind farm is significantly less than the summation of the power generated by each turbine when operating as a standalone entity. This power reduction can be attributed to the energy loss due to the wake effects – the resulting velocity deficit in the wind downstream of a turbine. In the case of wind farm design, the wake losses are generally quantified using wake models. The effectiveness of wind farm design (seeking to maximize the farm output) therefore depends on the accuracy and the reliability of the wake models. This paper compares the impact of the following four analytical wake models on the wind farm power generation: (i) the Jensen model, (ii) the Larsen model, (iii) the Frandsen model, and (iv) the Ishihara model. The sensitivity of this impact to the Land Area per Turbine (LAT) and the incoming wind speed is also investigated. The wind farm power generation model used in this paper is adopted from the Unrestricted Wind Farm Layout Optimization (UWFLO) methodology. Single wake case studies show that the velocity deficit and the wake diameter estimated by the different analytical wake models can be significantly different. A maximum difference of 70% was also observed for the wind farm capacity factor values estimated using different wake models

Keywords: Capacity factor, Land Area per Turbine, power generation, Unrestricted Wind Farm Layout Optimization, velocity deficit, wake model

Nomenclature

U	Incoming wind speed (m/s)
D	Rotor diameter (m)
H	Hub height (m)
D_{wake}	Wake diameter (m)
u_{def}	Velocity deficit (m/s)
s	Normalized downstream distance from the turbine
r	Normalized radial distance from the turbine
I_a	Ambient turbulence intensity

*Doctoral Student, Multidisciplinary Design and Optimization Laboratory, Department of Mechanical and Aerospace Engineering. AIAA Student Member
†Doctoral Student, Multidisciplinary Design and Optimization Laboratory, Department of Mechanical, Aerospace and Nuclear Engineering. AIAA Student Member
‡Distinguished Professor and Department Chair. Department of Mechanical and Aerospace Engineering. AIAA Lifetime Fellow. Corresponding author. Email: messac@syr.edu

I. Introduction

Increasing social and scientific concern for environmental issues has led to an appreciable growth in wind energy installation. Currently, wind energy is one of the most cost-effective renewable sources of new electricity generation. However, there remains significant scope for improvement of wind power generation technologies. In this paper, we will focus on how wake models affect the efficiencies of wind farm design technologies.

A. Wind Farm Power Generation

As wind flows across an individual turbine, the power available (P) in the wind is given by,

$$P = \frac{1}{2}\rho A U^3 \tag{1}$$

where ρ is the air density; A is the rotor swept area; and U is the uniform incoming wind speed at hub height.

Two important information can be observed from the above equation:

1. the power available to a wind turbine is proportional to the area swept by the rotor.
2. the power available to a wind turbine is proportional to the cube of the wind speed immediately in front of the turbine.

In practice, it is important to note that the power output continues to increase with wind speed until the wind speed reaches the turbine rated speed; wind turbines maintain their power output at the rated capacity above the rated speed (up to the cut-out speed).

In the case of *wind farm design*, it is challenging to predict the power generation of a wind farm, owing to the complexity of wind flow inside the farm. Because wind farms generally consist of multiple wind turbines located in a particular arrangement over a substantial stretch of land (onshore) or water body (offshore).[1] Factors that influence the power generation of a wind farm are primarily the environmental condition and the farm design.

Environmental conditions include the variation in wind conditions, namely wind speed, wind direction, and air density.[2] Farm design factors include turbine characteristics (*e.g.*, hub height, rotor diameter), placement of turbines, and land configuration. The power loss in a farm site can be minimized if the placement of turbines is optimized. Significant work has been done in the wind farm layout optimization using various algorithms to minimize the power loss.

A layout-based power generation model is used in this paper to compute the power output of a wind farm. This power generation model, developed in the Unrestricted Wind Farm Layout Optimization (UWFLO) methodology,[3] is used to quantify the power generation as a function of the turbine characteristics, turbine coordinates, and incoming wind speed. An influence matrix is also created to identify if a turbine is in the wake from upstream turbines. For a $N-$turbine wind farm, Turbine-j is in the influence of the wake created by Turbine-i if and only if

$$\begin{gathered} \Delta x_{ij} < 0 \; and \; \sqrt{(\Delta y_{ij})^2 + (\Delta H_{ij})^2} - \tfrac{D_j}{2} < \tfrac{D_{wake,ij}}{2}, \\ \Delta x_{ij} = x_i - x_j, \; \Delta y_{ij} = y_i - y_j, \; \Delta H_{ij} = H_i - H_j \\ \forall i, j = 1, 2, \ldots, N, i \neq j \end{gathered} \tag{2}$$

where the index i or j indicates the corresponding turbine number; x and y represent the turbine coordinates; D_j and H_j represent the rotor diameter and the hub height, respectively; and $D_{wake,ij}$ represents the width of wake (created by Turbine-j) at the location of Turbine-j. C_P is the power coefficient.

In this paper, the *generalized power curve* is used to derive the power coefficient.[4] This *generalized power curve* is scaled back to represent the approximate power response of a particular commercial turbine, using its specifications, as given by:

$$\frac{P}{P_r} = \begin{cases} P_n\left(\frac{U-U_{in}}{U_r-U_{in}}\right), & if \; U_{in} < U < U_r \\ 1, & if \; U_r < U < U_{out} \\ 0, & if \; U_{out} < U \; or \; U < U_{in} \end{cases} \tag{3}$$

where P_r is the rated capacity of turbine; U_{in}, U_{out}, and U_r are turbine's cut-in, cut-out, and rated speed, respectively; and P_n represents the polynomial fit for the *generalized power curve*. Therefore, the power coefficient (C_P) can be expressed as

$$C_P = \frac{P}{k_g k_b \left(\frac{1}{2}\rho\pi\frac{D_j}{4}U^3\right)} \tag{4}$$

where ρ is the air density; and parameters k_g and k_b represent the mechanical efficiency and the electrical efficiency, respectively.

The induction factor of a wind turbine is defined as the fractional decrease in wind speed between the freestream velocity and the rotor plane. Most of the popular wind farm power generation models assume a constant induction factor over the entire wind farm.[4] In practice, the wake expansion and the power reduction due to the wake effect are strongly related to the induction factor. To this end, a variable induction factor is used in this power generation model. According to the 1-D flow assumption, the induction factor a and the power coefficient C_P can be related by

$$C_P = 4a(1-a)^2 \tag{5}$$

Thrust coefficient, C_T, is also related to the induction factor, as given by

$$C_T = 4a(1-a) \tag{6}$$

Additionally, the Katic's model[5] is used to account for the velocity deficit due to wake merging. If Turbine-j is in the influence of multiple wakes created by K upstream turbines, the corresponding velocity deficit u_j is given by

$$u_j = \sqrt{\sum_{k=1}^{K} \frac{A_{kj}}{A_j}\left(U - U_{kj}\right)^2} \tag{7}$$

where A_{kj} is the effective influence area of wake (created by Turbine-k) on Turbine-j. If Turbine-j is completely in the wake of Turbine-k, $A_{kj} = A_j$; otherwise, A_{kj} denotes the overlapping area between the wake of Turbine-k and Turbine-j.

The net power generation of a wind farm, P_{farm}, is given by

$$P_{farm} = \sum_{j=1}^{N} P_j \tag{8}$$

In this paper, we represent the power performance of the farm in terms of the capacity factor. The capacity factor of a wind farm is defined as the ratio of the actual power generation to the ideal power that the wind farm could generate if always operating at the nameplate capacity, which can be expressed as

$$\eta_{farm} = \frac{P_{farm}}{\sum_{j=1}^{N} P_{rj}} \tag{9}$$

where P_{rj} is the rated capacity of Turbine-j.

B. The Wake Effect

There are two major objectives involved in *optimal wind farm planning*: *(i)* maximizing the capacity factor, and/or *(ii)* minimizing the Cost of Energy (COE).[2] As wind flows across a wind turbine, the wind speed decreases and the turbulence intensity increases. Thus, a wake is formed behind the turbine, which affects downstream turbines. Not only does the wake continue to move in the downstream direction, it also expands laterally. As a result, downstream wind turbines that are not coaxially downstream can be affected by the upstream turbine wake as well. Collectively, this is called the wake effect. There are two major impacts of the wake effect: *(i)* it causes a deficiency in the overall energy due to the velocity deficit, and *(ii)* it causes a reduction of the turbine lifetime due to increased turbulence induced structural loading.[6] Because of the wake effect, turbines located downstream from other turbines always generate less energy, which causes the

actual energy produced from a wind farm to be less than the simple product of the energy extracted from each standalone turbine. To this end, an understanding of turbine wakes is crucial for *optimal wind farm planning*.

Intuitively, the power reduction due to the wake effect can be reduced if the spacing between turbines is increased, because turbine wakes recover with distance downstream. In practice, however, the turbine spacing cannot be infinitely large due to practical constraints on the land area of the site. Chowdhury et al.[2] characterized the influence of the Land Area per MW Installed (LAMI) and the Nameplate Capacity to characterize their influences on the optimal wind farm performance. In that method, the optimum land area could be determined if the number and the selection of turbines are given.

This paper is aimed to investigate the impact of using different wake models on wind farm power generation, and also to explore how sensitive this impact is to the Land Area per Turbine and the incoming wind speed. In a given wind farm, some turbines might be in the wake of upstream turbines based on the prediction of a particular wake growth model, and might not be under such wake influence based on another wake growth model. Such differences in estimated wake growth and wake speed can lead to significant differences in the estimated wind farm power generation when different wake models are used; and theses differences are strongly related to the Land Area per Turbine and the incoming wind speed.

II. Wake Models

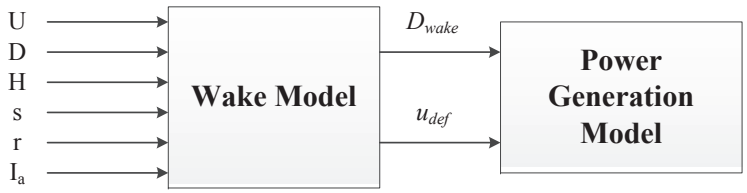

Figure 1. General inputs and outputs of an analytical wake model

Two types of wake models are commonly used to evaluate the power reduction: (i) analytical and (ii) computational wake models. In the analytical wake model (as shown in Figure 1), a set of analytical expressions are used to mathematically describe the behavior of turbine wakes. Computational wake models use complete Computational Fluid Dynamics (CFD) analysis (dictated by the Navier-Stokes equations) to characterize the flow more accurately. However, the use of the CFD-based wake primarily depends on the velocity immediately in front of it. In the case of wind farm layout optimization, the wake models need to simulate the wake behavior of all installed turbines for thousands of candidate farm layouts. Compared to CFD-based models, analytical models are thus preferred for their computational efficiency in wind farm layout optimization.

Wind turbine wakes typically can be divided into two types: the near wake and the far wake.[7] In the near wake, the turbine geometry determines the shape of the flow field.[?] The region under the near wake can be up to two to five rotor diameters downstream from the turbine, depending on the ambient turbulence.[8] Many studies have been conducted on modeling the near wake using either vortex wake models or generalized actuator disc models.[7,8] The far wake region starts once the shear layer approaches the center line, *i.e.*, the flow is fully developed. Compared to the near wake, the influence of the rotor blades can be neglected in the far wake; however, wake interactions, turbulence modeling, and the topographic effect become more important in the far wake.

Owing to the relevant assumptions made for the far wake, far wake models are very effective in modeling the wake expansion, as well as the velocity deficit. Moreover, in commercial wind farms, turbines are rarely placed so close to each other; that they will be in the near wake region (of each other). Therefore, far wake models are widely used in wind farm layout optimization problems, and are particularly investigated in this paper.

In the case of far wake modeling, two types of models are commonly considered: kinematic models (also called explicit models) and field models (or implicit models).[7] Field models evaluate the complete flow field or part of the flow field when the wind farm is regular (*e.g.*, axial symmetry). A turbulence model is also required in a field model to solve the Reynolds-averaged Navier-Stokes equations.[7] However, in a field model,

the flow magnitudes at every point need to be calculated. Also, some aspects of the flow behavior cannot be well predicted with a regular field; to that end, models that retain 3-dimensional effects are needed.[9] Compared to field models, kinematic wake models start the wake description after the wake has expanded, and are assigned an initial transverse velocity profile for the wake. The velocity deficit is usually obtained from global momentum conservation, and the wake growth is by the ambient turbulence and the turbulence created by the shear in the wake.[9] However, the change in ambient turbulence is not considered in kinematic models. Hence, a turbulence model has to be coupled with kinematic wake models in order to account for variable ambient turbulence (if needed) throughout the entire wind farm.

Considering the relatively low efficiency of field models and the nonnecessity of variable ambient turbulence (in most cases), kinematic wake models are sufficient for the estimation of wind farm power generation. Four kinematic wake models are investigated in this paper: Jensen model, Larsen model, Frandsen model, and Ishihara model. Table 1 lists the factors considered in each wake model. The description of each wake model will be presented in the following subsections.

Table 1. Inputs to each wake model

Input of wake model	Jensen's	Frandsen's	Larsen's	Ishihara's
Incoming wind speed	✓	✓	✓	✓
Downstream distance from the turbine	✓	✓	✓	✓
Radial distance from the turbine			✓	✓
Rotor diameter	✓	✓	✓	✓
Hub height			✓	
Turbulence intensity			✓	✓

A. Jensen Model

The analytical wake model developed by Jensen and later reported by Katic[5, 10] is one of the oldest analytical wake models. The key assumptions in this model are that the wake behind the wind turbine has a linear expansion, and the velocity deficit is only dependent on the distance downstream from the turbine. The wake growth is formulated as

$$D_{wake} = D(1 + 2ks) \tag{10}$$

where s is the normalized downstream distance (with respect to the rotor diameter) from the turbine. The velocity deficit u_{def} in the (fully developed) wake is expressed as

$$u_{def} = U_\infty \left[\frac{1 - \sqrt{1 - C_T}}{(1 + 2ks)^2} \right] \tag{11}$$

where the parameter k is the wake decaying constant, which represents how the wake breaks down by specifying the growth of the wake width per unit length in the downstream direction.

B. Larsen Model

The Larsen wake model was first recommended in the European Wind Turbine Standards II (EWTS II) 1999 report for use in wake load calculations.[11, 12] The derivation of this model is based on the Prandtl turbulent boundary layer equations. The closed-form solutions to the wake growth and the mean wake speed profile can be obtained by assuming a semi-similar velocity profile.

In this model, the Prandtl's mixing length theory is applied, and the wake flow is assumed to be incompressible, stationary and axisymmetric. The velocity deficit, depending on both the radial distance (r) and the downstream distance from the turbine (x), can be formulated as

$$u_{def} = -\frac{U_\infty}{9} \left[C_T A (x + x_0)^{-2} \right]^{\frac{1}{3}} \left\{ r^{\frac{3}{2}} \left[3c_1^2 C_T A (x + x_0) \right]^{-\frac{1}{2}} - \left(\frac{35}{2\pi} \right)^{\frac{3}{10}} (3c_1^2)^{-\frac{1}{5}} \right\}^2 \tag{12}$$

where A is the rotor swept area. The wake growth in the Larsen model is given by

$$D_{wake} = 2\left(\frac{35}{2\pi}\right)^{\frac{1}{5}}\left(3c_1^2\right)^{\frac{1}{5}}\left[C_T A(x+x_0)\right]^{\frac{1}{3}} \tag{13}$$

where c_1 is a constant that represents the non-dimensional mixing length (related to the Prandtl's mixing length); and x_0 is another constant that denotes the turbine's position with respect to the applied coordinate system. The formulae used to estimate these two constants are given by[13]

$$c_1 = \left(\frac{D_{eff}}{2}\right)^{\frac{5}{2}}\left(\frac{105}{2\pi}\right)^{-\frac{1}{2}}\left(C_T A x_0\right)^{-\frac{5}{6}} \tag{14}$$

$$x_0 = \frac{9.5D}{\left(\frac{2R_{9.5}}{D_{eff}}\right)^3 - 1} \tag{15}$$

where D_{eff} is the effective rotor diameter given by

$$D_{eff} = D\sqrt{\frac{1+\sqrt{1-C_T}}{2\sqrt{1-C_T}}} \tag{16}$$

and $R_{9.5}$ represents the wake radius at a relative distance of 9.5 rotor diameters ($9.5D$) downstream from the turbine. The blockage effect of the ground is also taken into account in this wake model; once the wake width exceeds the hub height as it expands along the downstream direction, it starts interacting with the ground. In the EWTS II report,[13] $R_{9.5}$ is defined as

$$R_{9.5} = 0.5\left[R_{nb} + min\left(H, R_{nb}\right)\right] \tag{17}$$

where R_{nb} is an empirical expression related to the ambient turbulence (I_a),

$$R_{nb} = max\left(1.08D, 1.08D + 21.7D\left(I_a - 0.05\right)\right) \tag{18}$$

C. Frandsen Model

The analytical wake model developed by Frandsen et al. is adopted in the Storpark Analytical Model (SAM).[14] The objective of SAM is to predict the wind speed deficit in large offshore wind farms with a rectangular site area and equal spacing of the wind turbines.

In the Frandsen model, the turbine wake is assumed to have three impacting regimes. In the first regime, the multiple-wake is dealt with in a single row of wind turbines. There are no mutual interactions between turbines, and the only possible effects are from physical boundaries (such as the ground). The second regime begins where two or more wakes meet and start interacting with each other. As a result of wake merging, the wake in this regime stops expanding laterally but continues only in the vertical direction. In the last regime, the wake flow tends to be in balance with the planetary boundary layer (PBL). Since the Frandsen model was aimed at predicting the wind speed deficit in large wind farms, the wake flow will be in balance with the PBL as long as the wind farm can be extended infinitely.

The wake growth in the first regime is given by

$$D_{wake} = D\left(\beta^{k/2} + \alpha s\right)^{1/k} \tag{19}$$

with the wake expansion parameter β formulated as

$$\beta = \frac{1+\sqrt{1-C_T}}{2\sqrt{1-C_T}} = \left(\frac{D_{eff}}{D}\right)^2, \quad s = x/D \tag{20}$$

where the parameter α describes the initial wake expansion. The value of k is 3 if the Schlichting solution to the wake expansion is chosen, and 2 if the square root shape is chosen.[14,15]

For the single wake case, the velocity deficit is formulated as

$$u_{def} = \frac{U_\infty}{2}\left(1 \pm \sqrt{1 - 2\frac{A}{A_{wake}}C_T}\right) \tag{21}$$

where A_{wake} is the wake impacting area corresponding to the wake width. In the "±" sign, the "+" applies to cases in which the induction factor $a \leq 0.5$, while the "−" applies to $a > 0.5$.

D. Ishihara Model

Ishihara et al.[16] developed an analytical wake model by using wind tunnel data for a scaled model of a Mitsubishi wind turbine. One important feature of this model is that it accounts for the effects of turbulence on the wake recovery from both the ambient turbulence and the mechanical generated turbulence. Experiments have shown that for onshore sites, the rate of the wake recovery is high due to the existence of sufficient turbulence in the wake. In the case of offshore sites, a relatively lower ambient turbulence intensity is prevalent; the wake recovery is therefore more dependent on the turbine-generated turbulence. It can be said that a wind turbine with a large thrust coefficient generally has a high wake recovery rate.[16–18]

The velocity profile of Ishihara model is assumed to have a Gaussian profile, and the velocity deficit is given by

$$u_{def} = \frac{\sqrt{C_T}U_\infty}{32}\left(\frac{1.666}{k_1}\right)^2\left(\frac{x}{D}\right)^{-p}\exp\left(-\frac{r^2}{{D_{wake}}^2}\right) \tag{22}$$

where the wake growth is formulated as

$$D_{wake} = \frac{k_1 {C_T}^{\frac{1}{4}}}{0.833}D^{1-\frac{p}{2}}x^{\frac{p}{2}} \tag{23}$$

The parameter p is a function of turbulence intensity, as given by

$$p = k_2(I_a + I_w) \tag{24}$$

where I_a and I_w represent the ambient turbulence and the turbine-generated turbulence, respectively. The turbine-generated turbulence can be expressed as

$$I_w = \frac{k_3 C_T}{max(I_a, 0.03)}\left\{1 - \exp\left[-4\left(\frac{x}{10D}\right)^2\right]\right\} \tag{25}$$

The coefficients k_1, k_2, and k_3 are respectively set to 0.27, 6.0, and 0.004 as found in the literature.[16,17]

III. Investigation of Analytical Wake Models

The power output of a wind farm is a complex function of the incoming wind conditions, and the location and features of the turbines in the farm. It is typical to use wake models to quantify the flow characteristics inside the farm and subsequently estimate the power generation. However, for a given wind condition, using different wake models would result in different predictions of the wind farm power generation. The purpose of this paper is to investigate the impact of using different wake models on the estimation of wind farm power generation.

A. Single Wake Test

The single wake test provides insightful information to help understand how key factors affect the wake velocity deficit and the wake growth behind a turbine. In this section, the single wake test is conducted for each wake model, assuming a flat terrain. The GE $2.5MW - 100m$ turbine is used for the single wake test. The specification of this turbine is given in Table 2. The ambient turbulence and the turbine thrust

Table 2. GE $2.5MW - 100m$ Turbine

Specifications	Value
Rotor diameter	100 m
Hub height	100 m
Cut-in	3.0 m/s
Cut-out	25 m/s
Rated speed	12.5 m/s

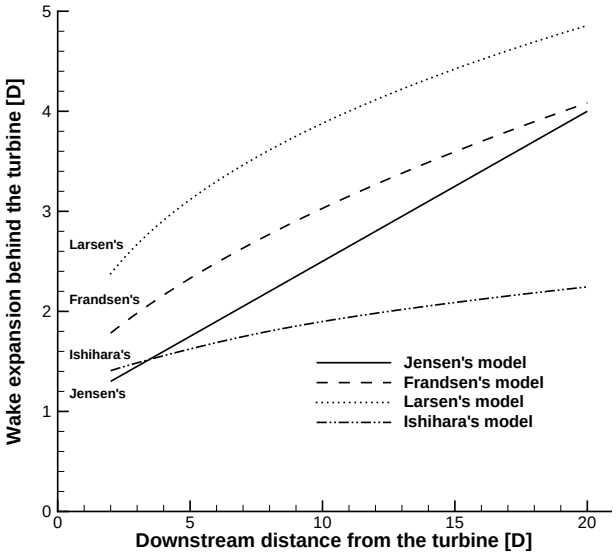

Figure 2. Wake growth behind a GE $2.5MW - 100m$ wind turbine

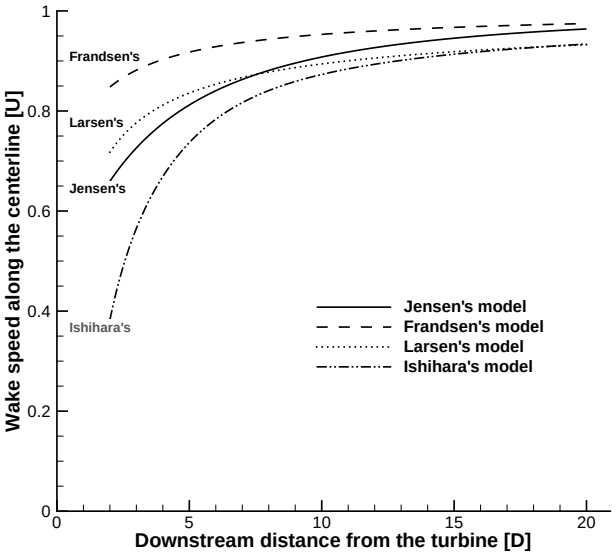

Figure 3. Wake speed behind a GE $2.5MW - 100m$ wind turbine

coefficient are assumed to be constant at 0.13 and 0.82 (onshore), respectively. Additionally, since far wake scenarios are considered, the wake simulation starts at two rotor diameters downstream from the turbine.

Figures 2 and 3 show the wake growth and the wake speed behind the GE $2.5MW - 100m$ turbine predicted by the four different analytical wake models (investigated in this paper). It is observed that, through the entire flow field, the Frandsen model predicts the highest wake speed and the Larsen model predicts the largest wake diameter. Since an effective rotor diameter is assumed in these two models, they also predict a larger initial wake expansion than that predicted by the other two models. The Ishihara model predicts the lowest wake speed; however, it yields the highest rate of wake recovery. This phenomenon can be attributed to the greater mixing of the wake with the upper layers of the Atmospheric Boundary Layer (ABL), which is facilitated by the turbine generated turbulence (distinctly accounted for in the Ishihara model).

B. Effect of Wake Models on Wind Farm Power Generation

1. Description of Numerical Experiments

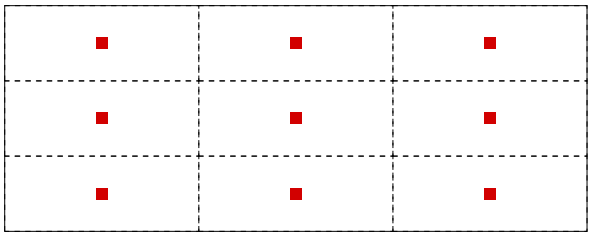

Figure 4. A gird-like wind farm with 9 installed GE $2.5MW - 100m$ turbines

The purpose of this paper is to investigate the impact of using different wake models on the wind farm power generation. The wake growth and the wake speed primarily depend on the velocity immediately in front of the turbine and the downstream distance from the turbine. Through the single wake test, it indicates that the wake behavior predicted by each wake model is significantly different. Numerical experiments are also conducted in this paper to understand the influences of the incoming wind speed and the Land Area per Turbine (LAT) on the wind farm power generation.

A grid-like wind farm with 9 GE $2.5MW - 100m$ installed turbines is used for the numerical experiments, as shown in Fig. 4. The incoming wind is assumed to have a uniform velocity profile over the rotor area, and a fixed direction (from left to right). The range of incoming wind speed studied varies between the cut-in speed and the cut-out speed. In order to characterize the spacing between turbines, the Land Area per MW Installed is selected as an independent parameter, which varies in the following range[2]

$$10\frac{D^2}{P_r} < A_{MW} < 30\frac{D^2}{P_r} \tag{26}$$

where P_r is the rated power in MW. Therefore, the numerical range of the total land area for the concerned wind farm is specified as

$$360,000\ m^2/MW \leq A_{farm} \leq 1,080,000\ m^2/MW \tag{27}$$

The spacing between turbines is assumed to be uniform, such that the Land Area per Turbine is given by

$$40,000\ m^2/MW \leq A_{turbine} \leq 120,000\ m^2/MW \tag{28}$$

Assuming the wind farm has a rectangular shape, a fixed aspect ratio of $\frac{7}{3}$ is specified.[1] The downstream spacing is ranged from $5D$ to $20D$, while the lateral spacing is no less than $2D$. Since turbines are uniformly located, the ratio of the downstream spacing to the lateral spacing is also constrained at $\frac{7}{3}$. The ambient turbulence intensity is fixed at 0.13.

C. Results and Discussion

1. Power Variation with the Land Area per Turbine

Figures 5(a) − 5(f) show the variation of the capacity factor with the Land Area per Turbine (LAT), obtained for different values of incoming wind speed. Among the four analytical wake models, the Frandsen model predicts the highest capacity factor while the Ishihara wake model predicts the lowest capacity factor. Three scenarios are observed based on the flow patterns inside the wind farm.

In the first scenario, the incoming wind speed is very small, and the power is mostly generated from the turbines located on the first row (as shown in Fig. 4). Other downstream turbines do not start due to the wake is lower than the cut-in speed. As shown in Fig. 5(a), with an incoming wind speed of $4m/s$, the LAT does not affect the capacity factor predicted by the Jensen model until it reaches 27 hectares, where the wake speed recovers enough to drive downstream turbines. The capacity factor predicted by the Frandsen model has been already influenced by the LAT at a relatively low incoming wind speed, because the Frandsen

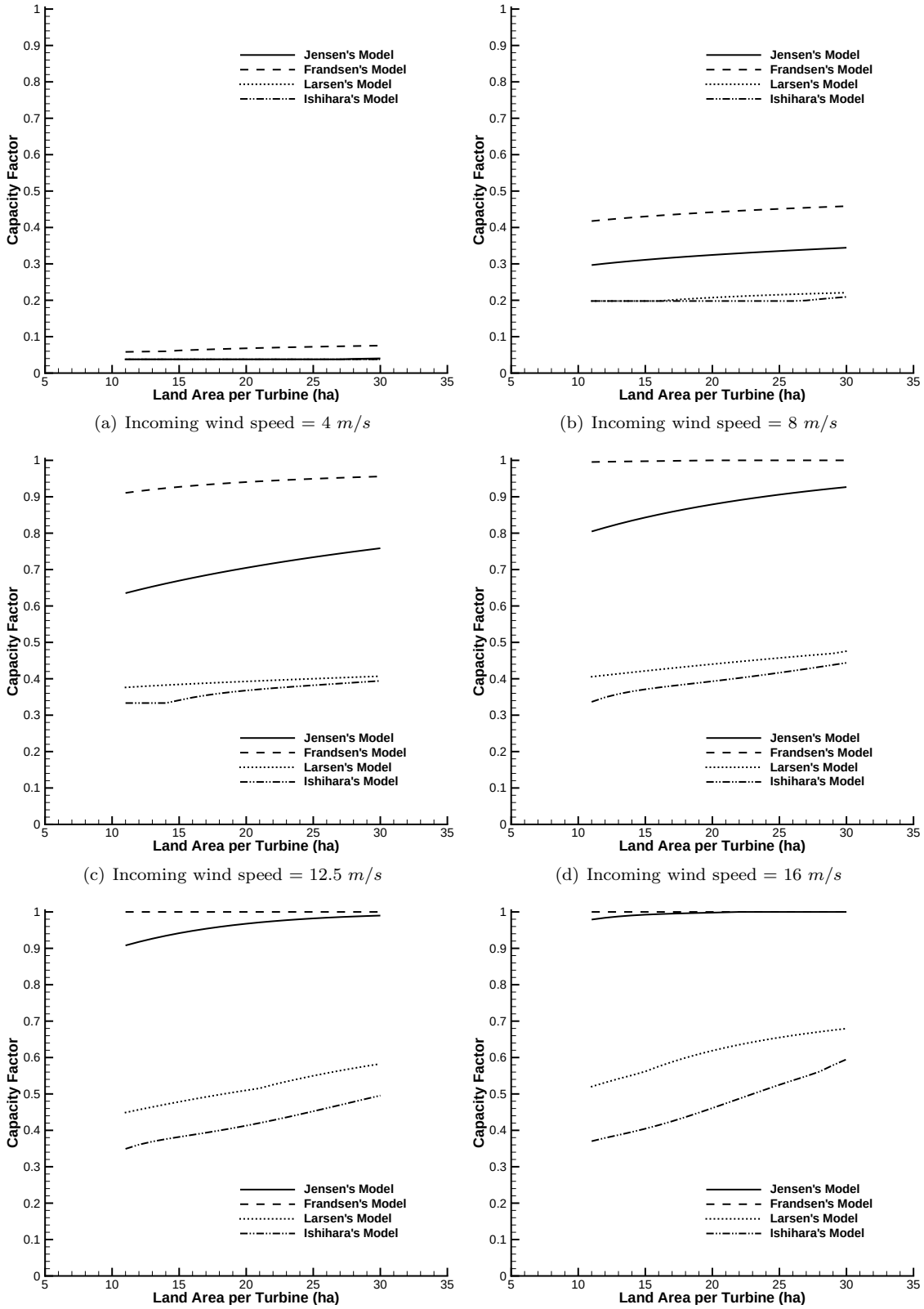

(a) Incoming wind speed = 4 m/s

(b) Incoming wind speed = 8 m/s

(c) Incoming wind speed = 12.5 m/s

(d) Incoming wind speed = 16 m/s

(e) Incoming wind speed = 20 m/s

(f) Incoming wind speed = 24 m/s

Figure 5. Variation of the capacity factor with the Land Area per Turbine

model predicts the highest wind speed and a relatively small wake diameter, as shown in the single wake test (2). However, the LAT has no impact on the capacity factor predicted by either the Larsen model or the Ishihara model, since both of them predict relatively low wake speeds.

In the second scenario, the wake speed in front of downstream turbines is significantly higher than the turbine cut-in speed. The flow patterns inside the wind farm become more complex in this case owing to the influences from the wake effect and the LAT. As shown in Fig. 5(b), the LAT starts to affect the capacity factor predicted by all the four wake models at an incoming speed of $8m/s$. It also can be observed that the capacity factor improves as the LAT increases. This trend can be seen more clearly in Fig. 5(c). Interestingly, the LAT starts influencing the capacity factor predicted by the Ishihara wake model at a higher incoming wind speed, compared to that predicted by the other three wake models. This phenomenon can be attributed to the relatively lower wake speeds predicted by the Ishihara model. Even at a relatively high incoming wind, the capacity factor predicted by the Ishihara model starts being affected at a large value of LAT (approximately 26 hectares). It is also interesting to note that the Jensen model predicts lower wake speed than that predicted by the Larsen model up to $7D$ distance downstream from the turbine. However, the LAT starts influencing the capacity factor predicted by the Jensen model at a lower incoming speed than it does for the Larsen model. This phenomenon is attributed to the relatively larger wake diameter predicted by the Larsen model, which causes more power reduction for the downstream turbines.

A third scenario can be observed when the first row of turbines reach their rated capacity. As the incoming wind speed increases, the wake speed becomes higher than the rated speed in this case. Therefore, the power generated from downstream turbines reaches the rated capacity, leading to a 100% capacity factor. As shown in Fig. 5(d) and 5(e), the capacity factor predicted by the Frandsen model has reached 100%. As shown in Fig. 5(f), the Jensen model also predicts a 100% capacity factor. The difference in the capacity factor predicted by the Larsen model and by the Ishihara model decreases as the LAT increases, since the predicted wake speeds of those two models are close to each other when the downstream distance is large, as shown in Fig. 3. However, due to the larger wake diameter predicted by the Larsen model, it leads to a lower rate of capacity factor increase with LAT than that yielded by the Ishihara model.

2. Power Variation with the Incoming Wind Speed

The variations of the capacity factor with the incoming wind speed is investigated at selected values of the LAT are shown in Fig. 6(a) − 6(d). Among the four analytical wake models, we observe that the Frandsen model predicts the highest capacity factor while the Ishihara wake model predicts the lowest capacity factor. This result is similar to that of the single wake test as shown in Fig. 3. For a given value of the LAT, the incoming wind speed required by the Frandsen model to reach a 100% capacity factor is lower than that required by the other wake models.

IV. Conclusions

This paper investigates the impact of four analytical wake models on the estimated power output of a wind farm. The influences of the Land Area per Turbine (LAT) and the incoming wind speed on the wind farm capacity factor, in the context of using different wake models, are also investigated. For incoming wind speeds lower than the turbine rated speed, the farm capacity factors is observed to increase with increasing LAT, irrespective of the type of wake model used. However, for incoming wind speed significantly higher than the rated speed, some wake models (*e.g.*, Frandsen model) yield a constant farm capacity factor with changing LAT (within the specified ranges); the other wake models still exhibit increasing capacity factor with increasing LAT. The observation of constant capacity factor (with increasing LAT), for incoming wind speeds higher than the turbine rated speed, can be attributed to the difference in incoming wind speed and the rated speed being greater than the maximum velocity deficit in the wind farm (predicted by the Frandsen model). When using different wake models, the maximum difference in the predicted farm capacity factor reached a value of nearly 70% within the specified ranges of incoming wind speed and LAT. These observations indicate that the knowledge of the comparative behavior of different wake models is crucial in determining the reliability of wind farm designs obtained using these models.

Further research can focus on the comparison of the optimal wind farm performance obtained when using different wake models. The influence of land shape on the wind farm power generation, in the context of using different wake models, can also be explored in the future.

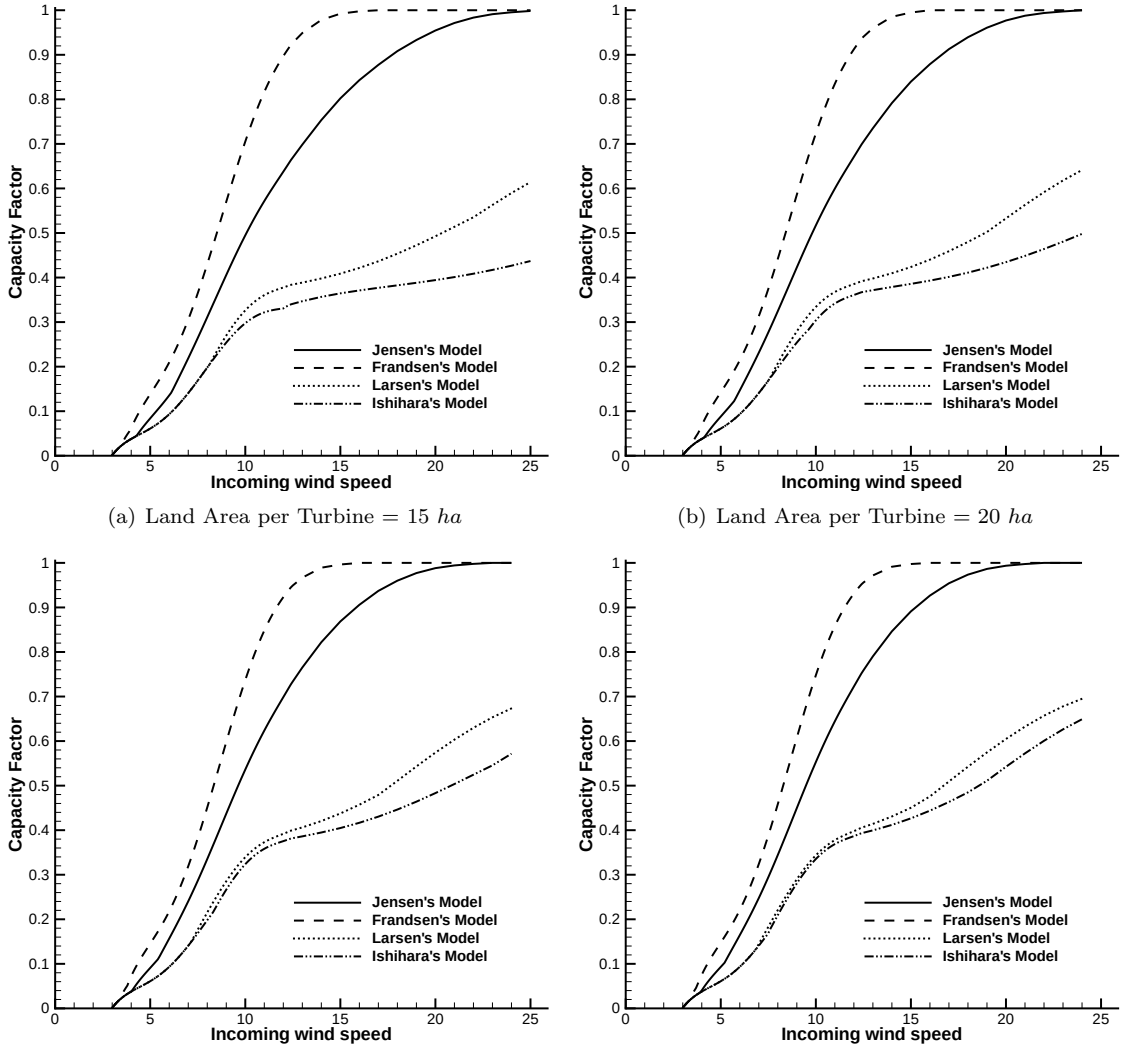

(a) Land Area per Turbine = 15 ha

(b) Land Area per Turbine = 20 ha

(c) Land Area per Turbine = 25 ha

(d) Land Area per Turbine = 30 ha

Figure 6. Variation of the capacity factor with the incoming wind speed

V. Acknowledgements

Support from the National Science Foundation Awards CMMI-1100948, and CMMI-0946765 is gratefully acknowledged. Any opinions, findings, and conclusions or recommendations expressed in this paper are those of the authors and do not necessarily reflect the views of the NSF.

References

[1]Chowdhury, S., Zhang, J., Messac, A., and Castillo, L., "Characterizing The Influence of Land Configuration on The Optimal Wind Farm Performance," *ASME 2011 International Design Engineering Technical Conferences (IDETC)*, ASME, Washington, DC, August 28-31 2011.

[2]Chowdhury, S., Zhang, J., Messac, A., and Castillo, L., "Characterizing The Influence of Land Area and Nameplate Capacity on The Optimal Wind Farm Performance," *ASME 2012 6th International Conference on Energy Sustainability*, ASME, San Diego, July 23-26 2012.

[3]Chowdhury, S., Zhang, J., Messac, A., and Castillo, L., "Unrestricted Wind Farm Layout Optimization (UWFLO): Investigating Key Factors Influencing The Maximum Power Generation," *Renewable Energy*, Vol. 38, No. 1, 2012, pp. 16–30.

[4]Chowdhury, S., *Integrative modeling and Novel Particle Swarm-based Optimal Design of Wind Farms*, Ph.D. thesis, Rensselaer Polytechnic Institute, Troy, New York, July 2012.

[5]Katic, I., Hojstrup, J., and Jensen, N., "A Simple Model for Cluster Efficiency," *European Wind Energy Association Conference and Exhibition '86*, EWEA, A. Raguzzi, Rome, October 1987, pp. 407–410.

[6]Steinfeld, G., "Wind Energy Meteorology: Modeling of wind turbines wakes," Tech. rep., ForWind - Center for wind energy research, Carl von Ossietzky University of Oldenburg, June 2011.

[7]Renkema, D., *Validation of wind turbine wake models using wind farm data and tunnel measurements*, Master's thesis, Delft University of Technology, June 2007.

[8]Castillo, L., "Wind Turbine Array and Turbulence," Tech. rep., Rensselaer Polytechnic Institute, Troy, NY, July 2011.

[9]Vermeer, L., Sorensen, J., and Crespo, A., "Wind turbine wake aerodynamics," *Aerospace Sciences*, Vol. 39, No. 6-7, August-October 2003, pp. 467–510.

[10]Jensen, N., "A Note on Wind Generator Interaction," Tech. rep., Riso National Laboratory, Roskilde, Denmark, November 1983.

[11]Larsen, G., Hojstrup, J., and Madsen, H., "Wind Fields in Wakes," *EWEC'96*, Goteborg, Sweden, 1996, pp. 764–768.

[12]Larsen, G., "A Simple Wake Calculation Procedure," Tech. rep., Riso National Laboratory, Roskilde, Denmark, December 1983.

[13]Pierik, J., Dekker, J., Braam, H., Bulder, B., Winkelaar, D., Larsen, G., Morfiadakis, E., Chaviaropoulos, P., Derrick, A., and Molly, J., "European wind turbine standards II," *Wind energy for the next millennium Proceedings*, edited by E. Petersen, P. Jensen, K. Rave, P. Helm, and H. Ehmann, 1999 European Wind Energy Conference, James and James Science Publishers, Nice, March 1999, pp. 568–571.

[14]Frandsen, S., Barthelmie, R., Pryor, S., Rathmann, O., Larsen, S., Hojstrup, J., and Thogersen, M., "Analytical Modelling of Wind Speed Deficit in Large Offshore Wind Farms," *Wind Energy*, Vol. 9, No. 1-2, January-April 2006, pp. 39–53.

[15]Barthelmie, R. J., Folkerts, L., Larsen, G. C., Rados, K., Pryor, S. C., Frandsen, S. T., Lange, B., and Schepers, G., "Comparison of Wake Model Simulations withy Offshore Wind Turbine Wake Profiles Measured by Sodar," *Atmospheric and Oceanic Technology*, Vol. 23, No. 7, July 2006, pp. 888–901.

[16]Ishihara, T., Yamaguchi, A., and Fujino, Y., "Development of a New Wake Model Based on a Wind Tunnel Experiment," Tech. rep., Global Wind, 2004.

[17]Mittal, A. and Sreenivas, K., "Investigation of Two Analytical Wake models Using Data From Wind Farms," ASME 2011 International Mechanical Engineering Congress and Exposition, Denver, November 2011.

[18]Crasto, G. and Gravdahl, A., "CFD wake modeling using a porous disc," Tech. rep., WindSim, Tonsberg, Norway, 2009.